Design and Performance Analysis of Super-Twisting Algorithm Control for Direct-Drive PMSG Wind Turbine Feeding a Water Pumping System

Benzaouia Soufyane[1,2(✉)], Zouggar Smail[1], Rabhi Abdelhamid[2], and Mohammed Larbi Elhafyani[1]

[1] Laboratory of Electrical Engineering and Maintenance – LEEM, High School of Technology, University Mohammed 1st, Oujda, Morocco
soufyane.benzaouia@gmail.com

[2] Laboratory of Modelisation, Information and Systems – MIS, University of Picardie Jules Verne, 33 rue Saint Leu, 80039 Amiens, Cedex, France

Abstract. This paper deals with the nonlinear control of a direct-drive *PMSG* wind turbines using the super-twisting algorithm. The studied system is assumed supplying a water pumping system for the use in isolated sites and areas. The aim of the proposed control strategy is tracking the wind turbine maximum power point. The designed controllers are based on one of the high-order sliding mode controller (*HOSM*) versions, which is the super-twisting algorithm. This latter possess many attractive features as the chattering-free behavior, finite time convergence, less information demand, simplicity, stability and robustness against external disturbances. The performance of the whole system in closed-loop mode is assessed through computer simulations.

Keywords: Wind energy · Water pumping system · Super-twisting algorithm · Nonlinear systems · PMSG · MPPT · Sliding mode controller

1 Introduction

In recent decades, wind energy has received a lot of attention as one of the clean alternative energy sources [1]. In general, renewable energies aim to reduce the negative impact of conventional electricity sources on the environment and also supplying remote areas and isolated sites where access to the classical energy is difficult. Water pumping is one of the principal renewable energy application; photovoltaic energy is the most used and preferred for water supply. In some cases and for some locations, solar energy cannot be the best solution. Wind energy has recently been adopted as a solution for regions with good wind potential. In literature, many wind electric water pumping configurations and control strategies have been proposed and studied [2–4]. The main goal of the existed studies is ensuring an optimal and a maximum efficiency of the water pumping system operation. The studied configuration in this paper is shown in Fig. 1. It consists of permanent-magnet synchronous generator, a controlled

A. El Moussati et al. (Eds.): SmartICT 2019, LNEE 684, pp. 271–281, 2020.
https://doi.org/10.1007/978-3-030-53187-4_31

AC/DC converter connected to a permanent-magnet *DC* motor driving a centrifugal pump (nonlinear load).

The permanent-magnet synchronous generator (*PMSG*) is one of the most preferred choice for standalone systems due to its high efficiency, self-excitation features, reliability and also for allowing a direct-drive systems avoiding by that the use of a gearbox [5]. The major drawbacks of wind energy conversion systems (*WECS*) is the highly nonlinear behavior [1]. Figure 2.b represent the power coefficient $\left(C_p\right)$ as function of the pitch angle (β) and the specific speed (λ), and Fig. 2.a shows the mechanical power as a function of rotor speed of the turbine for different values of wind speed. Maximizing the captured wind energy power is the main objective, many control strategies can be found in literature as well as controllers improvements in order to overcome the drawbacks of the conventional controllers. In [1], an adaptive fuzzy-*PI* control is considered to replace the conventional constant gains *PI* controller for *PMSG* vector control. A sliding mode control strategy is proposed in [6] and [7] for a *PMSG* controlled by vector control. In [8] a hybrid fuzzy sliding mode controller is proposed for controlling the permanent magnet synchronous generator speed. In [9], a general regression neural network (*GRNN*) controller is proposed for induction generator (*IG*) speed drive. A fuzzy neural network controller is proposed in [10] for the same generator kind. In [11], a hybrid intelligent *PMSG* control based on sliding mode controller combined with fuzzy inference mechanism and adaptive algorithm is proposed.

This paper presents the control of a direct-drive permanent-magnet synchronous generator wind turbine used in an autonomous water pumping system. The proposed optimal control of the *PMSG* wind turbine is based on super-twisting algorithm. The overall control functions of the wind electric water pumping system are developed including the maximization of the captured power. The presented control strategy allows an efficient operation of the system in a wide range of winds and aims to make the turbine operating on the curve corresponding to the maximum power point. Computer simulations are presented in order to validate and evaluated the performance of the adopted control strategy on the studied system.

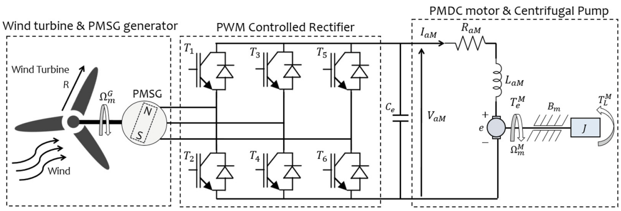

Fig. 1. Studied Wind Electric Water Pumping System.

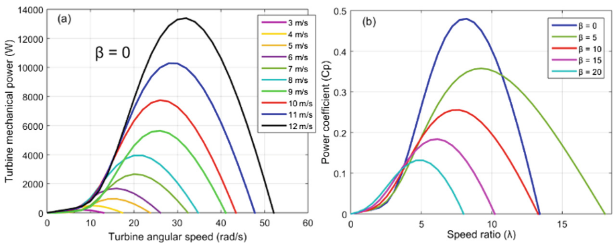

Fig. 2. a. Wind generator power curves at various wind speed, b. Characteristics C_p vs λ for different values of the pitch angle β.

2 Modeling of Wind Electric Water Pumping System

2.1 Modeling of the Wind Turbine

The model of the turbine is modeled from the following system equations [1, 5, 7]:

$$p_v = \frac{\left(\rho.A.v_w^3\right)}{2} \tag{1}$$

$$p_m = \frac{1}{2} C_p(\lambda, \beta).\rho.A.v_w^3 \tag{2}$$

$$\lambda = \frac{\Omega_m^G R}{v_w} \tag{3}$$

$$\begin{cases} C_p(\lambda, \beta) = C_1\left(\frac{C_2}{\gamma} - C_3.\beta - C_4\right)e^{\frac{-C_5}{\gamma}} + C_6.\lambda \\ \frac{1}{\gamma} = \frac{1}{\lambda + 0.08\beta} - \frac{0.035}{\beta^3+1} \end{cases} \tag{4}$$

$$C_1 = 0.5176, C_2 = 116, C_3 = 0.4, C_4 = 5, C_5 = 21$$

$$T_m^G = \frac{p_m}{\Omega_m^G} = \frac{1}{2.\Omega_m^G} C_p(\lambda, \beta).\rho.A.v_w^3 \tag{5}$$

$$\begin{cases} T_m^G = J^G \dot{\Omega}_m^G + f.\Omega_m^G + T_{em}^G \\ J^G = J_{turbine}^G + J_g^G \end{cases} \tag{6}$$

Where p_v is the wind power, ρ is the air density, A is the circular area, v_w is the wind speed, p_m is the mechanical power, C_p is the power coefficient, β is the pitch angle, λ is the tip speed ratio, Ω_m^G is the turbine rotor speed, R is the turbine radius, T_m^G is the mechanical torque, T_{em}^G is the electromagnetic torque produced by the generator, f is the friction coefficient and J^G is the total moment of inertia of the rotating parts.

2.2 Permanent Magnet Synchronous Generator (*PMSG*) Model

The *d*-*q* stator voltage equations of this generator are given by the following expressions [12, 18, 19]:

$$\begin{cases} V_{ds} = R_s I_{ds} + L_d \dot{I}_{ds} - \omega_r \psi_{qs} \\ V_{qs} = R_s I_{qs} + L_q \dot{I}_{qs} + \omega_r \psi_{ds} \\ \psi_{ds} = L_d I_{ds} + \psi_0 \\ \psi_{qs} = L_q I_{qs} \end{cases} \tag{7}$$

The differential equations of the *PMSG* can be obtained as follow:

$$\begin{cases} L_d \dot{I}_{ds} = V_{ds} - R_s I_{ds} + \omega_r L_q I_{qs} \\ L_q \dot{I}_{qs} = V_{qs} - R_s I_{qs} - \omega_r L_d I_{ds} - \psi_0 \omega_r \end{cases} \tag{8}$$

The electromagnetic torque is represented by:

$$T_{em}^{G} = \frac{3}{2} p \left[\left(L_d - L_q \right) I_{ds} I_{qs} + \psi_0 I_{qs} \right] \tag{9}$$

The *PMSG* is assumed to be wound-rotor, then $L_d = L_q$, and the expression of the electromagnetic torque in the rotor can be described as follow:

$$T_{em}^{G} = \frac{3}{2} p \psi_0 I_{qs} \tag{10}$$

Where L_d, L_q are the inductances of the generator on the q and d axis, R_s is the stator resistance, ψ_0 is the permanent magnetic flux, ω_r is the electrical rotating speed of the *PMSG* which is given by $\omega_r = p.\Omega_m^G$ and p is the number of pole pairs.

2.3 Permanent-Magnet *DC* Motor (*PMDC*) and Centrifugal Pump Model

The model of the *PMDC* motor is represented by the following equations [3]:

$$\begin{cases} V_{aM} = R_{aM} I_{aM} + L_{aM} \dot{I}_{aM} + e \\ T_e^M = K_t I_{aM} \\ e = K_e \Omega_m^M \\ T_e^M - T_L^M = J^M \dot{\Omega}_m^M + B_m . \Omega_m^M + T_f^M \end{cases} \tag{11}$$

The load torque of the centrifugal pump is given by the following expression:

$$T_L^M = a.\Omega_m^{M^n} + b \tag{12}$$

Where R_{aM} is the armature winding resistance, L_{aM} is the armature self-inductance, I_{aM} is the motor armature current, V_{aM} is the applied voltage, e is the back *e.m.f* of the *PMDC* motor, K_e is the voltage constant, Ω_m^M is the angular speed, K_t is the torque constant, J^M is the moment of inertia, B_m is the viscous torque constant, T_f^M is the torque constant for rotational losses, T_e^M, T_L^M are the electromagnetic torque and load torque respectively, and a, b are the constants of the pump.

3 *PMSG* Side Converter Control

In order to control the generator speed, a vector control strategy is applied to the *AC/DC* converter (Fig. 3). The generator speed Ω_m^G can be controlled by adjusting the electromagnetic torque (T_{em}^G) to its reference ($T_{em}^{G^*}$). That can be done by acting on the q-axis current (I_{qs}) using the equation $I_{qs}^* = \frac{2}{3p\psi_0} T_{em}^{G^*}$. The d-axis stator current (I_{ds}) component is forced to zero to achieve the maximum torque of the generator [12, 18]. The optimal reference rotational speed is calculated using $\Omega_{mopt}^G = \frac{\lambda^*.v_w}{R}$ where λ^* represents the optimum tip-speed ratio.

- **Super Twisting Algorithm (*STA*)**

The major known drawback associated with variable structure control implementation is the chattering phenomenon [13]. The most used technique to avoid this problem is the approach known as high-order sliding mode (*HOSM*). This latter is very well known in their stability and robustness against external disturbances and uncertainty. The increasing information demand is the main problem of the high-order sliding mode controllers; the implementation of the rth-order controller requires the knowledge of $\sigma, \dot{\sigma}, \ddot{\sigma}, \ldots, \sigma^{(r-1)}$ (σ is the sliding surface). The super-twisting algorithm is the exception, it has two main advantages. The first one is that the ST algorithm can be applied to any system having a relative degree equal to 1 with respect to sliding variable, and the second and the important advantage is that the ST algorithm does not require any information on the time derivative of the sliding variable and maintains all the distinctive robust features of the *SMC* [14, 15].

- ***Outer STA Generator Speed Controller***

The sliding surface for the *STA* speed controller is given as follows:

$$\sigma_{\Omega_m^G} = \Omega_{mopt}^G - \Omega_m^G \tag{13}$$

It follows that

$$\begin{cases} \dot{\sigma}_{\Omega_m^G} = \dot{\Omega}_{mopt}^G - \dot{\Omega}_m^G = \dot{\Omega}_{mopt}^G - \frac{T_m^G - f.\Omega_m^G - T_{em}^G}{J^G} \\ \ddot{\sigma}_{\Omega_m^G} = \varrho_1(t,x) + \Upsilon_1(t,x)\dot{T}_{em}^{G^*} \end{cases} \tag{14}$$

Where $\varrho_1(t,x)$ and $\Upsilon_1(t,x)$ are uncertain bounded functions that satisfy

$$\varrho_1(t,x) > 0, |\varrho_1(t,x)| > \Phi_1, 0 < \Gamma_{m1} < \Upsilon_1 < \Gamma_{M1} \tag{15}$$

The proposed second-order sliding mode control has been designed using the super twisting algorithm. The control law contains two parts, one is the continuous function of the sliding surface ($\sigma_{\Omega_m^G}$) and, the other, is the integral of a discontinuous control action [20]:

$$T_{em}^{G^*} = \upsilon_1 + \upsilon_2 \tag{16}$$

Where:

$$\begin{cases} \dot{\upsilon}_1 = -\alpha_1 sign\left(\sigma_{\Omega_m^G}\right) \\ \upsilon_2 = -\beta_1 \left|\sigma_{\Omega_m^G}\right|^{\rho} sign\left(\sigma_{\Omega_m^G}\right) \end{cases} \tag{17}$$

Using the Eqs. (10) and (16), the final *STA* speed controller is given as follows:

$$I_{qs}^* = \frac{2}{3p\psi_0}\left(-\beta_1 \left|\sigma_{\Omega_m^G}\right|^{\rho} sign\left(\sigma_{\Omega_m^G}\right) - \int \alpha_1 sign\left(\sigma_{\Omega_m^G}\right) dt\right) \tag{18}$$

Where α_1, β_1andρ are design parameters. To ensure the sliding manifolds convergence to zero in finite time, the gains can be chosen as follows [16]:

$$\begin{cases} \alpha_1 > \frac{\Phi_1}{\Gamma_{m1}} \\ \beta_1^2 \geq \frac{4\Phi_1}{\Gamma_{m1}^2} \frac{\Gamma_{M1}(\alpha_1 + \Phi_1)}{\Gamma_{m1}(\alpha_1 - \Phi_1)} \\ 0 < \rho \leq 0.5 \end{cases} \tag{19}$$

- ***Inner STA Current Controllers***

In order to regulate currents components I_{qs} and I_{ds} to their references (I_{ds}^* and I_{qs}^*), the sliding surfaces were chosen as follow:

$$\begin{cases} \sigma_{I_{ds}} = I_{ds}^* - I_{ds} \\ \sigma_{I_{qs}} = I_{qs}^* - I_{qs} \end{cases} \tag{20}$$

It follows that

$$\begin{cases} \dot{\sigma}_{I_{ds}} = \dot{I}_{ds}^{*} - \dot{I}_{ds} \\ \ddot{\sigma}_{I_{ds}} = \varrho_2(t,x) + \Upsilon_2(t,x)\dot{V}_{ds}^{*} \end{cases} and \begin{cases} \dot{\sigma}_{I_{qs}} = \dot{I}_{ds}^{*} - \dot{I}_{qs} \\ \ddot{\sigma}_{I_{qs}} = \varrho_3(t,x) + \Upsilon_3(t,x)\dot{V}_{qs}^{*} \end{cases} \tag{21}$$

Where $\varrho_2(t,x)$, $\varrho_3(t,x)$, $\Upsilon_2(t,x)$ and $\Upsilon_3(t,x)$ are uncertain bounded functions that satisfy

$$\begin{cases} \varrho_2(t,x) > 0, |\varrho_2(t,x)| > \Phi_2, 0 < \Gamma_{m2} < \Upsilon_2 < \Gamma_{M2} \\ \varrho_3(t,x) > 0, |\varrho_3(t,x)| > \Phi_3, 0 < \Gamma_{m3} < \Upsilon_3 < \Gamma_{M3} \end{cases} \tag{22}$$

The proposed second-order sliding mode control has been designed using the super twisting algorithm. The control voltages of q and d axis are defined as follow:

$$\begin{cases} V_{ds}^{*} = \mu_1 + \mu_2 - Fem_d \\ V_{qs}^{*} = w_1 + w_2 + Fem_q \end{cases} \tag{23}$$

Where:

$$\begin{cases} \dot{\mu}_1 = -\alpha_2 sign(\sigma_{I_{ds}}) \\ \mu_2 = -\beta_2|\sigma_{I_{ds}}|^{\rho} sign(\sigma_{I_{ds}}) \\ Fem_d = p\Omega_m^G L_q I_{qs} \end{cases} and \begin{cases} \dot{w}_1 = -\alpha_3 sign(\sigma_{I_{qs}}) \\ w_2 = -\beta_3|\sigma_{I_{qs}}|^{\rho} sign(\sigma_{I_{qs}}) \\ Fem_q = p\Omega_m^G(L_d I_{ds} + \psi_0) \end{cases} \tag{24}$$

Fem_d and Fem_q are the compensation terms.

The final inner *STA* current controllers are given as follow:

$$\begin{cases} V_{ds}^{*} = -\beta_2|\sigma_{I_{ds}}|^{\rho} sign(\sigma_{I_{ds}}) - \int \alpha_2 sign(\sigma_{I_{ds}})dt - p\Omega_m^G L_q I_{qs} \\ V_{ds}^{*} = -\beta_3|\sigma_{I_{qs}}|^{\rho} sign(\sigma_{I_{qs}}) - \int \alpha_3 sign(\sigma_{I_{qs}})dt + p\Omega_m^G(L_d I_{ds} + \psi_0) \end{cases} \tag{25}$$

Where α_i, β_i and ρ $(i = 2, 3)$ are design parameters. To ensure the sliding manifolds convergence to zero in finite time, the gains can be chosen as follows [16]:

$$\begin{cases} \alpha_i > \frac{\Phi_i}{\Gamma_{mi}} \\ \beta_i^2 \geq \frac{4\Phi_i}{\Gamma_{mi}^2}\frac{\Gamma_{Mi}(\alpha_i + \Phi_i)}{\Gamma_{mi}(\alpha_i - \Phi_i)}, (i = 2, 3). \\ 0 < \rho \leq 0.5 \end{cases} \tag{26}$$

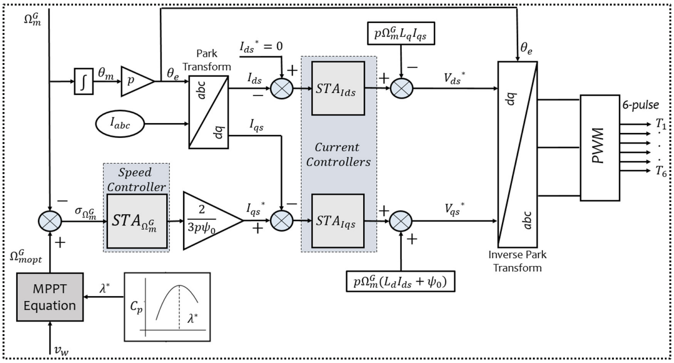

Fig. 3. Applied super-twisting algorithm based *MPPT* control

4 Results and Discussion

The following results were obtained for the studied wind electric water-pumping system described in Fig. 1 using *Matlab/Simulink* software. The control strategy was performed under variable wind speed profile. The wind speed was modeled as a sum of deterministic several harmonics [17].

$$v_w(t) = 7 + 0.2\sin(0.1047t) + 2\sin(0.2665t) + \sin(1.2930t) + 0.2\sin(3.6645t) \tag{27}$$

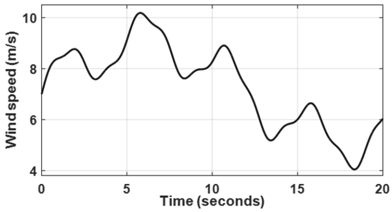

Fig. 4. Applied wind speed profile.

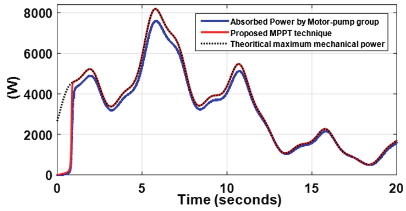

Fig. 5. Variation of the turbine mechanical power and the electrical absorbed power by the motor-pump.

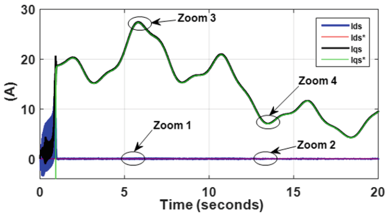

Fig. 6. *d-q* axis stator currents components.

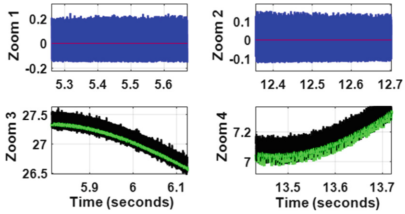

Fig. 7. Zoom of *d-q* axis stator currents components.

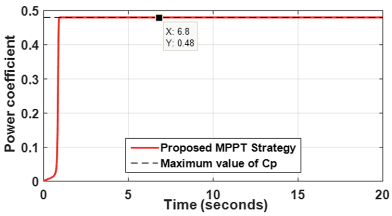

Fig. 8. Power coefficient and its optimal reference

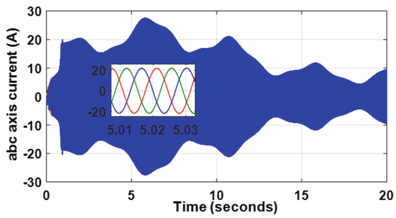

Fig. 9. *abc* axis current evolution.

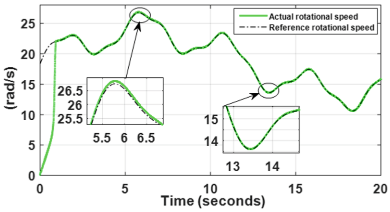

Fig. 10. Actual rotor speed and its reference (optimal).

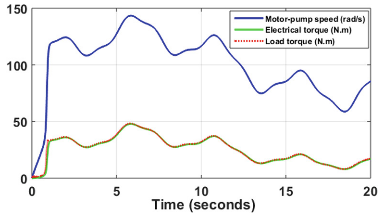

Fig. 11. Motor-pump performances.

The applied wind speed profile is shown in Fig. 4. The used waveforms contains two regions, the high wind speed range and the low one. Figure 5 illustrate the variation of the turbine mechanical power and the electrical absorbed power by the motor-pump group. The obtained results shows a good tracking performance of the maximum mechanical power. The dynamic difference between the mechanical turbine power and the electrical absorbed power is due to system inertia, friction and losses at converter and generator level. It is observed also on Fig. 8 that the power coefficient $\left(C_p\right)$ has been kept at its maximum value 0.48 even under random wind speed profile.

The *PMSG* vector control can be verified by observing the d and q current axis. Figures 6 and 7 show a good pursuit of the reference q current axis $\left(I_{qs}^*\right)$ generated by the outer super twisting algorithm controller, similarly to the d current component $\left(I_{ds}\right)$, it can been seen on the same figures that the I_{ds} remains around its reference (zero). Figure 9 shows that generator currents are sinusoidal, no harmonics or perturbations are observed at generator level, the thing that will increase the system efficiency. Figure 10 shows a good tracking performance of the speed rotor to the reference (optimal) speed with a very small error.

Figure 11 illustrates the motor-pump performances; it shows the evolution of the permanent-magnet *DC* motor speed, the electrical torque produced by the dc motor and the load torque opposed by the centrifugal pump.

5 Conclusion

In this paper, a wind electric water pumping system based on direct-drive *PMSG* wind turbine and *PMDC* motor connected to a centrifugal pump is studied and presented. A vector control strategy based on super-twisting algorithm controllers has been designed and evaluated under varying wind conditions. The obtained results proved the effectiveness and the robustness of the proposed control strategy on the studied system. The selected super-twisting algorithm has shown a good stability without chattering effects. The main advantage of the presented control strategy is that the *ST* algorithm requires only knowledge of the sign of the sliding variable, which means an easier implementation and good performances with less information demand. The proposed control strategy can be improved by replacing the mechanical sensors with observers state in order to reduce the overall system cost.

Acknowledgment. This research was supported by the National Center for Scientific and Technical Research (CNRST) of Morocco and the Embassy of France in Morocco.

References

1. Aissaoui, A.G., et al.: A fuzzy-PI control to extract an optimal power from wind turbine. Energy Convers. Manag. **65**, 688–696 (2013)
2. Ouchbel, T., et al.: Power maximization of an asynchronous wind turbine with a variable speed feeding a centrifugal pump. Energy Convers. Manag. **78**, 976–984 (2014)
3. Soufyane, B., et al.: A comparative investigation and evaluation of maximum power point tracking algorithms applied to wind electric water pumping system. In: International Conference on Electronic Engineering and Renewable Energy. Springer, Singapore (2018)
4. Lara, D., Merino, G., Salazar, L.: Power converter with maximum power point tracking MPPT for small wind-electric pumping systems. Energy Convers. Manag. **97**, 53–62 (2015)
5. Abdullah, M.A., et al.: A review of maximum power point tracking algorithms for wind energy systems. Renew. Sustain. Energy Rev. **16**(5), 3220–3227 (2012)
6. Emna, M.E., Adel, K., Mimouni, M.F.: The wind energy conversion system using PMSG controlled by vector control and SMC strategies. Int. J. Renew. Energy Res. **3**(1), 41–50 (2013)
7. Errami, Y., Ouassaid, M., Maaroufi, M.: A performance comparison of a nonlinear and a linear control for grid connected PMSG wind energy conversion system. Int. J. Electr. Power Energy Syst. **68**, 180–194 (2015)
8. Chen, C.H., Hong, C.-M., Ou, T.-C.: Hybrid fuzzy control of wind turbine generator by pitch control using RNN. Int. J. Ambient Energy **33**(2), 56–64 (2012)
9. Hong, C.-M., Cheng, F.-S., Chen, C.-H.: Optimal control for variable-speed wind generation systems using general regression neural network. Int. J. Electr. Power Energy Syst. **60**, 14–23 (2014)
10. Lin, W.-M., Hong, C.-M., Cheng, F.-S.: Fuzzy neural network output maximization control for sensorless wind energy conversion system. Energy **35**(2), 592–601 (2010)
11. Lin, W.-M., et al.: Hybrid intelligent control of PMSG wind generation system using pitch angle control with RBFN. Energy Convers. Manag. **52**(2), 1244–1251 (2011)
12. Dahbi, A., et al.: Realization and control of a wind turbine connected to the grid by using PMSG. Energy Convers. Manag. **84**, 346–353 (2014)

13. Valenciaga, F., Puleston, P.F.: High-order sliding control for a wind energy conversion system based on a permanent magnet synchronous generator. IEEE Trans. Energy Convers. **23**(3), 860–867 (2008)
14. Matraji, I., Al-Durra, A., Errouissi, R.: Design and experimental validation of enhanced adaptive second-order SMC for PMSG-based wind energy conversion system. Int. J. Electr. Power Energy Syst. **103**, 21–30 (2018)
15. Kunusch, C., et al.: Sliding mode strategy for PEM fuel cells stacks breathing control using a super-twisting algorithm. IEEE Trans. Control Syst. Technol. **17**(1), 167–174 (2008)
16. Mekri, F., Elghali, S.B., El Hachemi Benbouzid, M.: Fault-tolerant control performance comparison of three-and five-phase PMSG for marine current turbine applications. IEEE Trans. Sustain. Energy **4**(2), 425–433 (2012)
17. Tran, D.-H., et al.: Integrated optimal design of a passive wind turbine system: an experimental validation. IEEE Trans. Sustain. Energy **1**(1), 48–56 (2010)
18. Marmouh, S., Boutoubat, M., Mokrani, L.: Performance and power quality improvement based on DC-bus voltage regulation of a stand-alone hybrid energy system. Electr. Power Syst. Res. **163**, 73–84 (2018)
19. Mousa, H.H.H., Youssef, A.-R., Mohamed, E.E.M.: Variable step size P&O MPPT algorithm for optimal power extraction of multi-phase PMSG based wind generation system. Int. J. Electr. Power Energy Syst. **108**, 218–231 (2019)
20. Kunusch, C., Puleston, P.F., Mayosky, M.A., Dávila, A.: Efficiency optimisation of an experimental PEM fuel cell system via super twisting control. In: 2010 11th International Workshop on Variable Structure Systems (VSS), pp. 319–324. IEEE, June 2010